PAPER

Bit Error Rate Analysis of DS-CDMA with Joint Frequency-Domain Equalization and Antenna Diversity Combining

Fumiyuki ADACHI[†a)], ***Member and*** **Kazuaki TAKEDA**[†], ***Student Member***

SUMMARY To improve the DS-CDMA signal transmission performance in a frequency-selective fading channel, the frequency-domain equalization (FDE) can be applied, in which simple one-tap equalization is carried out on each subcarrier component obtained by fast Fourier transform (FFT). Equalization weights for joint FDE and antenna diversity combining based on maximal ratio combining (MRC), zero-forcing (ZF), and minimum mean square error (MMSE) are derived. The conditional bit error rate (BER) is derived for the given set of channel gains in a frequency-selective multipath fading channel. The theoretical average BER performance is evaluated by Monte-Carlo numerical computation method using the derived conditional BER and is confirmed by computer simulation. Performance comparison between DS- and multi-carrier (MC)-CDMA both using FDE is also presented.

key words: *DS-CDMA, frequency-domain equalization, antenna diversity, mobile radio*

1. Introduction

In next generation wireless communications systems, very high-speed data transmission is required under severe fading environments [1]. Frequency-selective multipath fading, encountered in a broadband wireless digital communication system, severely degrades the bit error rate (BER) performance [2], [3]. In direct sequence code division multiple access (DS-CDMA), well-known rake combining is applied to improve the BER performance [4]. However, as the spreading chip rate increases (or the spreading bandwidth becomes broader), the frequency-selectivity of the fading channel becomes severer due to increasing number of resolvable propagation paths. Accordingly, the increase in the inter-path interference (IPI) resulting from the asynchronism among different paths degrades the BER performance. Furthermore, the complexity of the rake receiver increases due to the increase in the number of rake fingers (or correlators) that are required for collecting enough signal power for data demodulation.

Recently, the combination of multi-carrier (MC) and CDMA, called MC-CDMA, has been attracting much attention for a broadband wireless multi-access and is under extensive study [5]–[9]. In MC-CDMA, each user's data-modulated symbol to be transmitted is spread over a number of orthogonal subcarriers using a spreading sequence defined in the frequency-domain. In an MC-CDMA receiver, simple one-tap frequency-domain equalization (FDE) is carried out on each received subcarrier component to improve the BER performance by exploiting the multipath channel frequency-selectivity.

Meanwhile, single-carrier wireless transmission with FDE is also gaining popularity [10]. Recently, it was shown by our computer simulation [11] that FDE can be applied to the reception of multi-code DS-CDMA signals in a severe frequency-selective fading channel to obtain the BER performance similar to that of MC-CDMA. Fast Fourier transform (FFT) is applied to decompose the received multi-code DS-CDMA signal into a number of subcarrier components (in this paper, the term "subcarrier" is used although subcarriers are not used for data modulation and the number of subcarriers equals to the FFT window size (or number of samples for FFT)) and FDE is carried out on each subcarrier component. Despreading can be done after performing inverse FFT (IFFT). In [11], the FFT window size equal to the spreading factor was assumed. However, it should be noted [12] that the spreading factor can be arbitrarily chosen irrespective of the FFT widow size. This suggests that FDE can also be applied to a multi-rate/multi-code DS-CDMA using orthogonal variable spreading factor (OVSF) codes [4]. In [13], it is shown that the FDE and despreading based on maximal ratio combining (MRC) is equivalent to the well-known rake combining. In addition to the use of FDE, antenna diversity reception is a powerful technique to further improve the BER performance in a frequency-selective fading channel [12] as in a frequency-nonselective fading channel. This is also true for MC-CDMA [14]. So far presented are only the simulation results to show how the use of FDE or joint use of FDE and antenna diversity reception improves the BER performance of DS-CDMA. To the best of author's knowledge, there has been no literature which theoretically treated the BER performance of DS-CDMA with joint FDE and antenna diversity reception.

This paper is intended to give a theoretical foundation to joint FDE and antenna diversity combining for the reception of DS-CDMA signals for the uncoded case. The remainder of this paper is organized as follows. Section 2 presents the transmission system model of DS-CDMA using joint FDE and antenna diversity combining. Then, equalization weights based on maximal-ratio combining (MRC), zero-forcing (ZF) and minimum mean square error combining (MMSE) are derived for joint FDE and antenna diversity combining in Sect. 3. An exrression for the conditional BER is derived for the given set of channel gains at different sub-

Manuscript received December 18, 2003.

Manuscript revised April 3, 2004.

[†]The authors are with the Dept. of Electrical and Communication Engineering, Graduate School of Engineering, Tohoku University, Sendai-shi, 980-8579 Japan.

a) E-mail: adachi@ecei.tohoku.ac.jp

carrier frequencies and, in Sect. 4, the theoretical average BER is evaluated by Monte-Carlo numerical computation method using the derived BER expression. In Sect. 5, the average BER performance is evaluated by computer simulation of the signal transmissions to confirm the theoretical analysis. Section 6 offers some conclusions and future work.

2. Transmission System Model

The data modulated symbol sequence is serial-to-parallel (S/P) converted into U parallel data streams $\{d_u(n);\ u = 0 \sim U-1\}$, which are then spread using U orthogonal spreading sequences $\{c_u(t);\ u = 0 \sim U-1\}$ having a spreading factor of SF. The resultant U chip sequences are summed and further multiplied by a scramble sequence $c_{scr}(t)$ to form the orthogonal multicode DS-CDMA signal, which is then divided into blocks of N_c chips. To apply FFT on the received DS-CDMA signals at the receiver, inserting the guard interval (GI) of N_g chips before transmission is necessary [11]–[13], similar to MC-CDMA, as shown in Fig. 1. Then, the time delayed signal is viewed as a circularly shifted version of the transmitted signal.

2.1 Transmit/Receive Signal Representation

Throughout this paper, T_c-spaced discrete time representation is used, where T_c represents the chip duration of the time-domain spreading codes. Without loss of generality, a time interval of $-N_g \le t < N_c$ is considered for the transmission of $(U/SF) \times N_c$ data symbols, where $U \le SF$. In this paper, we assume the square-root Nyquist chip shaping filter at the transmitter and the same filter at the receiver as the chip-matched filter. Also, ideal chip sampling timing is assumed at the receiver. The GI-inserted chip sequence $\tilde{s}(t)$ can be expressed using the equivalent lowpass representation as

$$\tilde{s}(t) = \sqrt{\frac{2E_c}{T_c}}\, s(t \bmod N_c), \tag{1}$$

where E_c is the chip energy per parallel data stream and

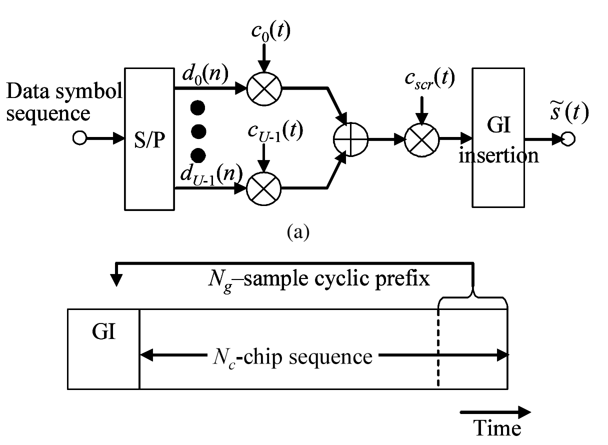

Fig. 1 Transmitter structure and GI insertion for DS-CDMA with FDE.

$$s(t) = \left[\sum_{u=0}^{U-1} d_u(\lfloor t/SF \rfloor)\, c_u(t \bmod SF)\right] c_{scr}(t) \tag{2}$$

with $|d_u(n)| = |c_u(t)| = |c_{scr}(t)|=1$, where $\lfloor x \rfloor$ is the largest integer smaller than or equal to x. The orthogonal spreading sequences and the scramble sequence have the following characteristics:

$$\begin{aligned}&\frac{1}{SF}\sum_{t=0}^{SF-1} c_u(t)c^*_{u'}(t) = \delta(u-u')\\ &E[c_{scr}(t)c^*_{scr}(\tau)] = \delta(t-\tau),\end{aligned} \tag{3}$$

where the asterisk denotes the complex conjugate operation, $\delta(x)$ the delta function, and $E[.]$ the ensemble average operation.

The transmitted signal is received via a frequency-selective fading channel. M-branch antenna diversity reception is considered. Assuming that the channel has L independent propagation paths with T_c-spaced distinct time delays $\{\tau_l;\ l = 0 \sim L-1\}$, the discrete-time impulse response $h_m(t)$ of the multipath channel experienced by the mth antenna is expressed as

$$h_m(t) = \sum_{l=0}^{L-1} h_{m,l}\delta(t-\tau_l), \tag{4}$$

where $h_{m,l}$ is the lth path gain with $\sum_{l=0}^{L-1} E[|h_{m,l}|^2] = 1$. Assuming block fading so that the path gains remain constant over one block interval of N_c chips, time dependency of the channel has been dropped for simplicity. It is assumed that the maximum time delay of the channel is shorter than GI. The received signal is sampled at the chip rate. The received signal on the mth antenna is

$$r_m(t) = \sum_{l=0}^{L-1} h_{m,l}\tilde{s}(t-\tau_l) + \eta_m(t), \tag{5}$$

where $\eta_m(t)$ is the additive white Gaussian noise (AWGN) process with zero mean and variance $2N_0/T_c$ with N_0 being the single-sided power spectrum density.

2.2 Joint FDE and Diversity Combining and Despreading

The receiver structure is illustrated in Fig. 2. After removal of GI, N_c-point FFT is applied to the received signal $r_m(t)$ to obtain

$$\begin{aligned}R_m(k) &= \sum_{t=0}^{N_c-1} r_m(t)\exp\left(-j2\pi k\frac{t}{N_c}\right)\\ &= \sqrt{\frac{2E_c}{T_c}} S(k)\sum_{l=0}^{L-1} h_{m,l}\exp\left(-j2\pi k\frac{\tau_l}{N_c}\right) + \Pi_m(k)\\ &= \sqrt{\frac{2E_c}{T_c}} S(k)H_m(k) + \Pi_m(k)\end{aligned} \tag{6}$$

for $0 \le k < N_c$, where $S(k)$, $H_m(k)$ and $\Pi_m(k)$ are the

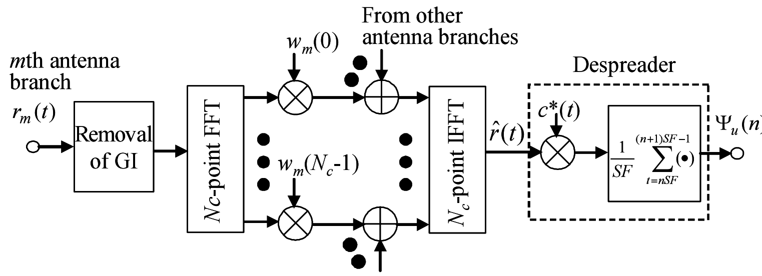

Fig. 2 Receiver structure using joint FDE and diversity combining and despreading.

kth subcarrier component of the orthogonal multicode DS-CDMA signal $s(t)$, the channel gain at the kth subcarrier frequency and the zero-mean noise sample having variance $2(N_0/T_c)N_c$ also at the kth subcarrier frequency, respectively. They are given by

$$\begin{aligned}S(k) &= \sum_{t=0}^{N_c-1} s(t)\exp\left(-j2\pi k\frac{t}{N_c}\right)\\ H_m(k) &= \sum_{l=0}^{L-1} h_{m,l}\exp\left(-j2\pi k\frac{\tau_l}{N_c}\right)\\ \Pi_m(k) &= \sum_{t=0}^{N_c-1} \eta_m(t)\exp\left(-j2\pi k\frac{t}{N_c}\right).\end{aligned} \tag{7}$$

Letting the equalization weight for the mth antenna be $w_m(k)$, the subcarrier component $\hat{R}(k)$ after equalization and diversity combining is given by

$$\begin{aligned}\hat{R}(k) &= \sum_{m=0}^{M-1} w_m(k)R_m(k)\\ &= \sqrt{\frac{2E_c}{T_c}}S(k)\hat{H}(k)+\hat{\Pi}(k),\end{aligned} \tag{8}$$

where $\hat{H}(k)$ and $\hat{\Pi}(k)$ are the equivalent channel gain and the noise component after joint FDE and antenna diversity combining, respectively, and are given by

$$\begin{aligned}\hat{H}(k) &= \sum_{m=0}^{M-1} w_m(k)H_m(k)\\ \hat{\Pi}(k) &= \sum_{m=0}^{M-1} w_m(k)\Pi_m(k).\end{aligned} \tag{9}$$

Then, N_c-point IFFT is performed on $\{\hat{R}(k); k=0\sim N_c-1\}$ to produce the time-domain signal $\{\hat{r}(t); t=0\sim N_c-1\}$:

$$\hat{r}(t) = \frac{1}{N_c}\sum_{k=0}^{N_c-1}\hat{R}(k)\exp\left(j2\pi t\frac{k}{N_c}\right). \tag{10}$$

Substitution of Eqs. (7) and (8) into Eq. (10), $\hat{r}(t)$ can be expressed as

$$\begin{aligned}\hat{r}(t) = &\sqrt{\frac{2E_c}{T_c}}\left(\frac{1}{N_c}\sum_{k=0}^{N_c-1}\hat{H}(k)\right)s(t)\\ &+\sqrt{\frac{2E_c}{T_c}}\frac{1}{N_c}\sum_{k=0}^{N_c-1}\hat{H}(k)\left[\sum_{\substack{\tau=0\\ \neq t}}^{N_c-1}s(\tau)\exp\left(j2\pi k\frac{t-\tau}{N_c}\right)\right]\\ &+\frac{1}{N_c}\sum_{k=0}^{N_c-1}\hat{\Pi}(k)\exp\left(j2\pi t\frac{k}{N_c}\right).\end{aligned} \tag{11}$$

The first term represents the desired signal component, the second the inter-chip interference (ICI) owing to IPI and the third the noise component. Note that the ICI is the sum of the interference from own spreading code (called self-interference) and from other spreading codes (called other code-interference).

Without loss of generality, detection of the nth data symbol of the uth data stream is considered. The despreader output for decision on $d_u(n)$ is given by

$$\Psi_u(n) = \frac{1}{SF}\sum_{t=nSF}^{(n+1)SF-1}\hat{r}(t)c^*(t), \tag{12}$$

where

$$c(t) = c_u(t \bmod SF)c_{scr}(t). \tag{13}$$

Substitution of Eq. (11) into Eq. (12) gives

$$\begin{aligned}\Psi_u(n) = &\sqrt{\frac{2E_c}{T_c}}\left(\frac{1}{N_c}\sum_{k=0}^{N_c-1}\hat{H}(k)\right)d_u(n)+\mu_{ICI}(n)\\ &+\mu_{noise}(n),\end{aligned} \tag{14}$$

where the first term represents the desired data symbol component and the second and third terms are ICI and noise due to AWGN, respectively. μ_{ICI} and μ_{noise} are given by

$$\begin{aligned}\mu_{ICI}(n) &= \frac{1}{SF}\sum_{t=nSF}^{(n+1)SF-1}c^*(t)\\ &\times\frac{1}{N_c}\sum_{k=0}^{N_c-1}\hat{H}(k)\left[\sqrt{\frac{2E_c}{T_c}}\sum_{\substack{\tau=0\\ \neq t}}^{N_c-1}s(\tau)\exp\left(j2\pi k\frac{t-\tau}{N_c}\right)\right]\\ \mu_{noise}(n) &= \frac{1}{SF}\sum_{t=nSF}^{(n+1)SF-1}c^*(t)\\ &\times\frac{1}{N_c}\sum_{k=0}^{N_c-1}\hat{\Pi}(k)\exp\left(j2\pi t\frac{k}{N_c}\right).\end{aligned} \tag{15}$$

3. Weights for Joint FDE and Antenna Diversity Combining

First, we consider MRC equalization weight and show that FDE using MRC is equivalent to rake combining [13]. Then, ZF equalization weight is obtained followed by MMSE equalization weight. ZF equalization is a special case of MMSE equalization.

3.1 MRC Equalization

We want to find the set of weights $\{w_m(k);\ m = 0 \sim M-1\}$ that maximizes the signal-to-noise power ratio (SNR) of $\Psi_u(n)$ for the given set of $\{H_m(k);\ m = 0 \sim M-1\}$. Since $\{\Pi_m(k);\ k = 0 \sim N_c-1$ and $m = 0 \sim M-1\}$ are the independent and identically distributed (i.i.d.) zero-mean complex-valued noise samples having variance $2(N_0/T_c)N_c$, SNR of $\Psi_u(n)$ is given by

$$SNR = \frac{\dfrac{2E_c}{T_c}\left|\dfrac{1}{N_c}\displaystyle\sum_{k=0}^{N_c-1}\hat{H}(k)\right|^2}{\sigma^2_{\mu_{noise}}} = 2\left(\frac{E_s}{N_0}\right)\frac{\left|\dfrac{1}{N_c}\displaystyle\sum_{k=0}^{N_c-1}\sum_{m=0}^{M-1}w_m(k)H_m(k)\right|^2}{\dfrac{1}{N_c}\displaystyle\sum_{k=0}^{N_c-1}\sum_{m=0}^{M-1}|w_m(k)|^2}, \tag{16}$$

where $\sigma^2_{\mu_{noise}} = (1/2)E[|\mu_{noise}|^2]$ and $E_s/N_0 = (E_c/N_0)SF$ is the average received symbol energy-to-AWGN power spectrum density ratio. Applying the Schwarz inequality for complex-valued numbers [15], the MRC weight that maximizes Eq. (16) is found to be

$$w_m^{MRC}(k) = H_m^*(k). \tag{17}$$

The MRC equalization enhances the frequency-selectivity of the channel and increases the ICI. Hence, it does not necessarily maximize the signal-to-interference plus noise power ratio (SINR), and degrades the BER performance [16].

From Eqs. (7), (8), and (17), Eq. (10) can be rewritten as

$$\begin{aligned}\hat{r}(t) &= \frac{1}{N_c}\sum_{k=0}^{N_c-1}\left(\sum_{m=0}^{M-1}H_m^*(k)R_m(k)\right)\exp\left(j2\pi t\frac{k}{N_c}\right)\\ &= \sum_{m=0}^{M-1}\sum_{l=0}^{L-1}h_{m,l}^*\left(\frac{1}{N_c}\sum_{k=0}^{N_c-1}R_m(k)\exp\left(j2\pi k\frac{t+\tau_l}{N_c}\right)\right)\\ &= \sum_{m=0}^{M-1}\sum_{l=0}^{L-1}h_{m,l}^*r_m(t+\tau_l).\end{aligned} \tag{18}$$

Hence, Eq. (12) becomes

$$\Psi_u(n) = \sum_{m=0}^{M-1}\sum_{l=0}^{L-1}h_{m,l}^*\hat{r}_{m,l}, \tag{19}$$

where

$$\hat{r}_{m,l} = \frac{1}{SF}\sum_{t=nSF}^{(n+1)SF-1}r_m(t+\tau_l)c^*(t) \tag{20}$$

is the correlator (or rake finger) output synchronized to the signal received via the lth propagation path associated with the mth antenna (this can be understood from Eq. (5)). Hence, the FDE using MRC and despreading is equivalent to the well-known rake combining.

The above discussion suggests [13] that the use of FDE provides the BER performance identical to the rake combining, but with the power penalty of a factor of $(1+N_g/N_c)$ due to GI insertion. In rake combining, the multipath channel must be resolved into L paths having different time delays and channel estimation is performed for coherent combining. If too many paths are present (or the channel frequency-selectivity is strong), the signal power of each path becomes small and consequently, channel estimation becomes difficult. Furthermore, the number of rake fingers should be increased as the number of paths increases. An advantage of FDE is that unlike rake combining, its complexity is independent of the degree of channel frequency-selectively. However, it should be pointed out that the GI length N_g must be longer than or equal to the maximum time delay difference of the channel and the block size N_c (or FFT window size) must be shorter enough so that the fading can be seen as block fading.

3.2 ZF Equalization

If the equivalent channel gain is made unity for all subcarriers, i.e.,

$$\hat{H}(k) = \sum_{m=0}^{M-1}w_m(k)H_m(k) = 1, \tag{21}$$

we have μ_{ICI}=0 in Eq. (15) and then Eq. (14) becomes

$$\Psi_u(n) = \sqrt{\frac{2E_c}{T_c}}d_u(n) + \mu_{noise}. \tag{22}$$

The orthogonality among different data streams can be completely restored. The weight that satisfies Eq. (21) is called the ZF weight, which is given by

$$w_m^{ZF}(k) = \frac{H_m^*(k)}{\displaystyle\sum_{m=0}^{M-1}|H_m(k)|^2}. \tag{23}$$

3.3 MMSE Equalization

The transmitted signal is given by Eq. (1). Its kth subcarrier component is given by

$$\tilde{S}(k) = \sqrt{\frac{2E_c}{T_c}}S(k). \tag{24}$$

However, the corresponding subcarrier component of the received signal is different from Eq. (24) and is given by Eq. (8). We define the equalization error at the kth subcarrier as

$$\begin{aligned}\varepsilon(k) &= \tilde{S}(k) - \hat{R}(k)\\ &= \sqrt{\frac{2E_c}{T_c}}S(k)\left(1-\sum_{m=0}^{M-1}w_m(k)H_m(k)\right)\\ &\quad -\sum_{m=0}^{M-1}w_m(k)\Pi_m(k).\end{aligned} \tag{25}$$

We want to find the set of equalization weights $\{w_m(k); m = 0 \sim M-1\}$ that minimizes the mean square error (MSE) $E[|\varepsilon(k)|^2]$ for the given set of $\{H_m(k); m = 0 \sim M-1\}$. It is assumed that the U data-modulated symbols $\{d_u(n); u = 0 \sim U-1\}$ are zero-mean and i.i.d. complex-valued random variables. Since $E[|S(k)|^2] = N_c U$ (this can be found from Eqs. (2) and (7)) and since $\Pi_m(k)$ is a zero-mean complex-valued noise sample having variance $2(N_0/T_c)N_c$, the MSE for the given set of $\{H_m(k); m = 0 \sim M-1\}$ becomes

$$E[|\varepsilon(k)|^2] = \frac{2E_c}{T_c}N_c U\left[\begin{array}{c} 1+\left|\sum_{m=0}^{M-1}w_m(k)H_m(k)\right|^2\\ -2\mathrm{Re}\left[\sum_{m=0}^{M-1}w_m(k)H_m(k)\right]\\ +\left(\frac{E_s}{N_0}\frac{U}{SF}\right)^{-1}\sum_{m=0}^{M-1}|w_m(k)|^2\end{array}\right]. \tag{26}$$

The set of weights that satisfy $\partial E[|\varepsilon(k)|^2]/\partial w_m(k) = 0$ for all m is the optimum one in the MMSE sense. Following [14], we obtain the following MMSE weight:

$$w_m^{MMSE}(k) = \frac{H_m^*(k)}{\sum_{m=0}^{M-1}|H_m(k)|^2+\left(\frac{U}{SF}\frac{E_s}{N_0}\right)^{-1}}, \tag{27}$$

which is identical to the MMSE weight for MC-CDMA [14]. When M=1 (no antenna diversity), Eq. (27) reduces to the MMSE weight shown in [17]. Removing the contribution of the noise (the second term of the denominator of Eq. (27)) gives the ZF weight of Eq. (23).

4. BER Analysis

The weights, derived in Sect. 3, for joint FDE and antenna diversity combining of DS-CDMA signals are identical to those of MC-CDMA [14]. In this section, we first theoretically derive the conditional BER based on Gaussian approximation of ICI and then, numerically evaluate the theoretical average BER performance. Finally, the performance comparison between DS- and MC-CDMA is presented. In the following analysis, as stated in Sect. 2, we assume block fading (i.e., the path gains stay constant over one block of N_c chips) and the maximum time delay of the channel being shorter than the GI length.

4.1 Expression for Conditional BER

It can be understood from Eq. (14) that the despreader output $\Psi_u(n)$ is a random variable with mean $\sqrt{2E_c/T_c}(N_c^{-1}\sum_{k=0}^{N_c-1}\hat{H}(k))d_u(n)$. Since the scramble sequence is used to make the resultant orthogonal multicode DS-CDMA signal white-noise like, i.e., $E[s(t)s^*(\tau)] = U\delta(t-\tau)$, μ_{ICI} can be approximated as a zero-mean complex-valued Gaussian noise. As a sequel, the sum of μ_{ICI} and μ_{noise} can be treated as a new zero-mean complex-valued Gaussian noise μ. The variance of μ is the sum of those of μ_{ICI} and μ_{noise}:

$$2\sigma_\mu^2 = E[|\mu|^2] = 2\sigma_{\mu_{ICI}}^2 + 2\sigma_{\mu_{noise}}^2, \tag{28}$$

where, from Appendix,

$$\begin{aligned}\sigma_{ICI}^2 &= \frac{1}{2}E[|\mu_{ICI}|^2]\\ &= \frac{U}{SF}\frac{E_c}{T_c}\left[\frac{1}{N_c}\sum_{k=0}^{N_c-1}\left|\hat{H}(k)\right|^2-\left|\frac{1}{N_c}\sum_{k=0}^{N_c-1}\hat{H}(k)\right|^2\right]\\ \sigma_{noise}^2 &= \frac{1}{2}E[|\mu_{noise}|^2]\\ &= \frac{1}{SF}\frac{N_0}{T_c}\left(\frac{1}{N_c}\sum_{k=0}^{N_c-1}\sum_{m=0}^{M-1}|w_m(k)|^2\right)\end{aligned} \tag{29}$$

for the given set of $\{H_m(k)$ and $w_m(k); k = 0 \sim N_c-1$ and $m = 0 \sim M-1\}$. Therefore, we have

$$\sigma_\mu^2 = \frac{1}{SF}\frac{N_0}{T_c}\times\left[\begin{array}{c}\frac{1}{N_c}\sum_{k=0}^{N_c-1}\sum_{m=0}^{M-1}|w_m(k)|^2+\left(\frac{U}{SF}\frac{E_s}{N_0}\right)\\ \cdot\left\{\frac{1}{N_c}\sum_{k=0}^{N_c-1}\left|\hat{H}(k)\right|^2-\left|\frac{1}{N_c}\sum_{k=0}^{N_c-1}\hat{H}(k)\right|^2\right\}\end{array}\right]. \tag{30}$$

We assume quaternary phase shift keying (QPSK) data-modulation and all "1" transmission (i.e., $d_u(n) = (1+j1)/\sqrt{2}$) without loss of generality. Since the ICI can be assumed to be circularly symmetric, the conditional BER for the given set of $\{H_m(k); m = 0 \sim M-1$ and $k = 0 \sim N_c-1\}$ (or equivalently, the given set of path gains $\{h_{m,l}; m = 0 \sim M-1$ and $l = 0 \sim L-1\}$) can be expressed as

$$\begin{aligned}p_b\left(\frac{E_s}{N_0},\{H_m(k)\}\right) &= \frac{1}{2}\mathrm{Prob}\left[\mathrm{Re}[\Psi_u(n)] < 0|\ \{H_m(k)\}\right]\\ &\quad+\frac{1}{2}\mathrm{Prob}\left[\mathrm{Im}[\Psi_u(n)] < 0|\ \{H_m(k)\}\right]\\ &= \frac{1}{2}erfc\left[\sqrt{\frac{1}{4}\gamma\left(\frac{E_s}{N_0},\{H_m(k)\}\right)}\right],\end{aligned} \tag{31}$$

where $erfc[x] = (2/\sqrt{\pi})\int_x^\infty \exp(-t^2)dt$ is the complementary error function and $\gamma\,(E_s/N_0, \{H_m(k)\})$ is the conditional SINR defined as

$$\gamma\left(\frac{E_s}{N_0}, \{H_m(k)\}\right) = \frac{2E_c}{T_c}\left|\frac{1}{N_c}\sum_{k=0}^{N_c-1}\hat{H}(k)\right|^2 \Big/ \sigma_\mu^2 = \frac{2\left(\frac{E_s}{N_0}\right)\left|\frac{1}{N_c}\sum_{k=0}^{N_c-1}\hat{H}(k)\right|^2}{\left[\begin{array}{l}\frac{1}{N_c}\sum_{k=0}^{N_c-1}\sum_{m=0}^{M-1}|w_m(k)|^2 + \left(\frac{U}{SF}\frac{E_s}{N_0}\right) \\ \cdot\left\{\frac{1}{N_c}\sum_{k=0}^{N_c-1}\left|\hat{H}(k)\right|^2 - \left|\frac{1}{N_c}\sum_{k=0}^{N_c-1}\hat{H}(k)\right|^2\right\}\end{array}\right]} \quad (32)$$

with $\hat{H}(k) = \sum_{m=0}^{M-1} w_m(k)H_m(k)$ and

$$w_m(k) = \begin{cases} H_m^*(k), & \text{for MRC} \\ \dfrac{H_m^*(k)}{\sum_{m=0}^{M-1}|H_m(k)|^2}, & \text{for ZF} \\ \dfrac{H_m^*(k)}{\sum_{m=0}^{M-1}|H_m(k)|^2 + \left(\frac{U}{SF}\frac{E_s}{N_0}\right)^{-1}}, & \text{for MMSE.} \end{cases} \quad (33)$$

The theoretical average BER can be numerically evaluated by averaging Eq. (31) over $\{H_m(k);\ m = 0 \sim M-1$ and $k = 0 \sim N_c - 1\}$:

$$P_b\left(\frac{E_s}{N_0}\right) = \int\cdots\int \frac{1}{2}erfc\left[\sqrt{\frac{1}{4}\gamma\left(\frac{E_s}{N_0}, \{H_m(k)\}\right)}\right] p(\{H_m(k)\})\prod_{m,k} dH_m(k), \quad (34)$$

where $p(\{H_m(k)\})$ is the joint probability density function (pdf) of $\{H_m(k);\ m = 0 \sim M-1$ and $k = 0 \sim N_c - 1\}$.

4.2 Lower Bounded BER

It can be understood from Eq. (32) that as the value of U/SF becomes smaller, the effect of ICI becomes less and less and thus, the achievable BER performance improves. A mathematically extreme case is when $U/SF \to 0$ (i.e., ICI is neglected). The maximum achievable conditional SINR is given by Eq. (32) with MRC equalization and $U/SF \to 0$. Substituting Eq. (17) and $U/SF = 0$ into Eq. (32), we have

$$\gamma_{\max}\left(\frac{E_s}{N_0}, \{H_m(k)\}\right) = 2\left(\frac{E_s}{N_0}\right)\frac{1}{N_c}\sum_{k=0}^{N_c-1}\sum_{m=0}^{M-1}|H_m(k)|^2. \quad (35)$$

An equivalent expression can be given, from Eq. (7), by

$$\gamma_{\max}\left(\frac{E_s}{N_0}, \{H_m(k)\}\right) = 2\left(\frac{E_s}{N_0}\right)\sum_{m=0}^{M-1}\sum_{l=0}^{L-1}\left|h_{m,l}\right|^2. \quad (36)$$

Denoting the pdf of $\alpha = \sum_{m=0}^{M-1}\sum_{l=0}^{L-1}\left|h_{m,l}\right|^2$ by $p(\alpha)$, the average BER is lower bounded as

$$P_{b,lower}\left(\frac{E_s}{N_0}\right) = \int_0^\infty \frac{1}{2}erfc\left[\sqrt{\alpha\frac{1}{2}\frac{E_s}{N_0}}\right]p(\alpha)d\alpha. \quad (37)$$

Let assume a frequency-selective Rayleigh fading channel having the uniform power delay profile. Then, $\{h_{m,l}\}$ are zero-mean and i.i.d. complex-valued Gaussian variables with the variance of $1/L$. The pdf of γ is given by [3]

$$p(\alpha) = \frac{L^{ML}}{(ML-1)!}\alpha^{ML-1}\exp(-\alpha L). \quad (38)$$

Thus, the lower bounded average BER is given by [3]

$$P_{b,lower}\left(\frac{E_s}{N_0}\right) = \left[\frac{1}{2}\left(1 - \sqrt{\frac{\frac{E_s}{N_0}}{\frac{E_s}{N_0} + 2L}}\right)\right]^{ML} \cdot\sum_{k=0}^{ML-1}\binom{ML-1+k}{k}\left[\frac{1}{2}\left(1 + \sqrt{\frac{\frac{E_s}{N_0}}{\frac{E_s}{N_0} + 2L}}\right)\right]^k, \quad (39)$$

where $\binom{a}{b}$ is the binomial coefficient. An approximate expression for the lower bounded average BER can be obtained for $E_s/N_0 \ggg 1$ as [3]

$$P_{b,\text{lower}}\left(\frac{E_s}{N_0}\right) \approx \left(\frac{E_s}{N_0}\right)^{-ML}\left(\frac{L}{2}\right)^{ML}\binom{2ML-1}{ML}, \quad (40)$$

which indicates that joint FDE and antenna diversity combining can achieve an ML-th order frequency diversity effect if the ICI effect can be neglected. However, due to ICI effect, the achievable BER performance degrades.

4.3 Theoretical and Simulation Results

The condition for the numerical evaluation of the theoretical average BER and the computer simulation is shown in Table 1. We assume a block length of N_c=256 (equal to the FFT window size), a GI length of N_g=32, and ideal coherent QPSK data modulation/demodulation. As a propagation channel, an L=16-path Rayleigh fading channel having the uniform power delay profile is considered (i.e., $\{h_{m,l}$;

Table 1 Simulation condition.

DS-CDMA	Block length	N_c=256
	Guard interval	N_g=32
	Data modulation	QPSK
Rayleigh fading channel	No. of paths	L=16
	Time delay difference	τ_l=l

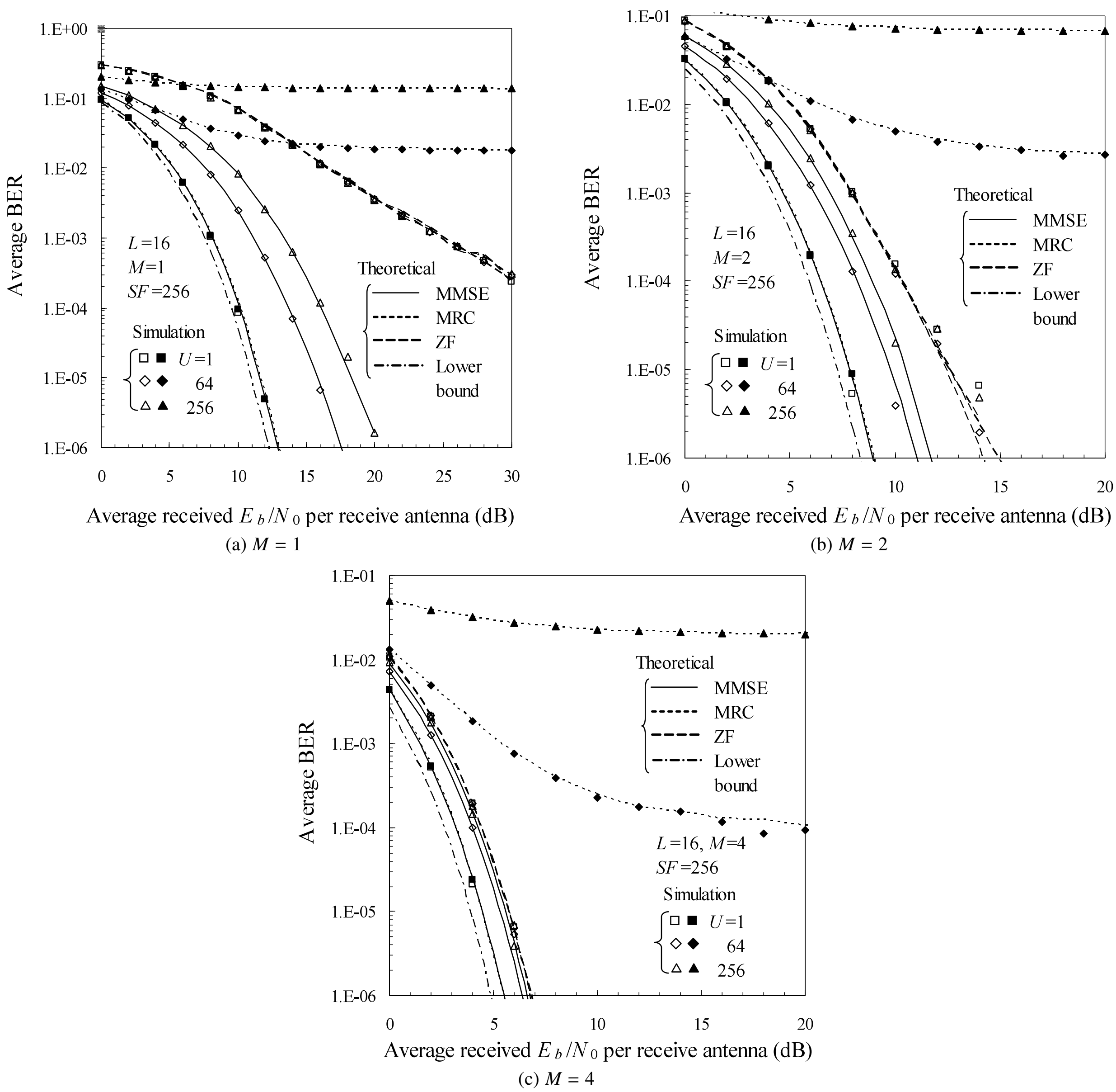

Fig. 3 Average BER performances using MMSE, MRC, and ZF equalizations as a function of the average received E_b/N_0 with U as a parameter. (a) M=1, (b) M=2, and (c) M=4.

$m = 0 \sim M-1$ and $l = 0 \sim L-1\}$ are zero-mean i.i.d. complex-valued Gaussian variables with a variance of $1/L$). It is assumed that the time delay of the lth path is $\tau_l = l$ chips and the maximum delay difference is less than the GI length (i.e., $L-1 \leq N_g$).

The numerical evaluation of the theoretical average BER is done by Monte-Carlo numerical computation method as follows. The set of path gains $\{h_{m,l};\ m = 0 \sim M-1$ and $l = 0 \sim L-1\}$ is generated for obtaining $\{H_m(k);\ k = 0 \sim N_c-1$ and $m = 0 \sim M-1\}$ using Eq. (7) and then $\{w_m(k);\ k = 0 \sim N_c-1$ and $m = 0 \sim M-1\}$ using Eq. (33). The conditional BER for the given average received E_s/N_0 is computed using Eq. (31). This is repeated sufficient number of times to obtain the theoretical average BER of Eq. (34).

Also presented below are the computer simulation results to confirm the validity of the theoretical analysis. In the simulation, an m-sequence with a repetition period of 4095 chips is used as the scramble sequence.

The theoretical average BER performance for MMSE, MRC and ZF equalizations is plotted as a function of the average received bit energy-to-the AWGN power spectrum density ratio E_b/N_0, which is defined as $E_b/N_0 = 0.5(E_s/N_0)(1+N_g/N_c)$, with U as a parameter in Fig. 3. For comparison, the lower bounded average BER performance given by Eq. (39) is also plotted. It can be seen that the MMSE equalization provides the best BER performance for all values of U. When U=1, the BER performance is almost identical for MRC and MMSE equalizations and the E_b/N_0 degradation for achieving BER=10^{-4} from the lower bound average BER performance becomes as small as 0.65 dB. Part of this E_b/N_0 degradation is due to the GI insertion loss of $10\log(8/7) = 0.58$ dB. However, as U increases, the BER performance degrades since the amount of ICI increases (this is clearly understood from Eq. (32)). The BER performance with ZF equalization is almost insensitive to U since no ICI is produced, but the performance is worse than with MMSE because of the noise enhancement as in MC-CDMA [5], [14]. On the other hand, with MRC equalization, the noise enhancement can be suppressed, but the large ICI is produced due to enhanced frequency-selectivity. Hence, the BER floor appears when $U > 1$. Note that no BER floor is produced in the MMSE and ZF equalizations. It can also be seen from Fig. 3 that the use of antenna diversity is powerful to improve the BER performance for all equalization schemes. The BER performance with ZF equalization consistently improves as M increases, but it is still worse than with MMSE equalization.

The computer simulated average BERs are plotted in Fig. 3 to compare with theoretical ones. A fairly good agreement with theoretical and computer simulated results is seen. This confirms the validity of our BER analysis based on the Gaussian approximation of ICI.

4.4 Comparison with MC-CDMA

We assume the number of subcarriers is equal to that of DS-CDMA (i.e., the FFT window size is equal for DS-CDMA and MC-CDMA). The kth subcarrier component $R_m^{MC}(k)$ of MC-CDMA signal received on the mth antenna can be expressed as

$$R_m^{MC}(k) = \sqrt{\frac{2E_c}{T_c}} S^{MC}(k)H_m(k) + \Pi_m(k), \tag{41}$$

where E_c and T_c are now the signal energy per FFT (or IFFT) sample per parallel data stream and the FFT sample period, respectively, and

$$S^{MC}(k) = \left[\sum_{u=0}^{U-1} d_u(\lfloor k/SF \rfloor) c_u(k \bmod SF)\right] c_{scr}(k). \tag{42}$$

The kth subcarrier component after equalization is given by

$$\begin{aligned}\hat{R}^{MC}(k) &= \sum_{m=0}^{M-1} w_m^{MC}(k) R_m^{MC}(k) \\ &= \sqrt{\frac{2E_c}{T_c}} S^{MC}(k)\hat{H}^{MC}(k) + \hat{\Pi}^{MC}(k),\end{aligned} \tag{43}$$

where $w_m^{MC}(k)$ is the equalization weight and

$$\begin{aligned}\hat{H}^{MC}(k) &= \sum_{m=0}^{M-1} w_m^{MC}(k) H_m(k) \\ \hat{\Pi}^{MC}(k) &= \sum_{m=0}^{M-1} w_m^{MC}(k) \Pi_m(k).\end{aligned} \tag{44}$$

The despreader output is expressed as

$$\Psi_u^{MC}(n) = \frac{1}{SF} \sum_{k=nSF}^{(n+1)SF-1} \hat{R}^{MC}(k) c^*(k), \tag{45}$$

which can be rewritten as

$$\begin{aligned}\Psi_u^{MC}(n) = &\sqrt{\frac{2E_c}{T_c}} \left(\frac{1}{SF} \sum_{k=nSF}^{(n+1)SF-1} \hat{H}^{MC}(k)\right) d_u(n) \\ &+ \mu_{ICI}^{MC}(n) + \mu_{noise}^{MC}(n).\end{aligned} \tag{46}$$

Equations (42), (43), (45) and (46) are equations corresponding to Eqs. (2), (8), (12) and (14) of DS-CDMA, respectively. This implies that the results for DS-CDMA can be applied to MC-CDMA with the replacement of N_c by SF. However, note that in Eq. (46), the second term represents the ICI (this represents the inter-code interference for MC-CDMA, although it is used to represent the inter-chip interference for DS-CDMA) from other spreading codes and hence, unlike DS-CDMA, no self-interference is present. This means that no ICI is present when $U=1$. On the other hand, since the self-interference is present in DS-CDMA, the ICI is present even when $U=1$. Referring to DS-CDMA analysis shown in Appendix and remembering that no self-interference is present in MC-CDMA, we have

$$\begin{aligned}\left(\sigma_{ICI}^{MC}\right)^2 &= \frac{U-1}{SF}\frac{E_c}{T_c}\left[\frac{1}{SF}\sum_{k=nSF}^{(n+1)SF-1}\left|\hat{H}(k)\right|^2 - \left|\frac{1}{SF}\sum_{k=nSF}^{(n+1)SF-1}\hat{H}(k)\right|^2\right] \\ \left(\sigma_{noise}^{MC}\right)^2 &= \frac{N_0}{T_c}\frac{1}{SF^2}\sum_{k=nSF}^{(n+1)SF-1}\sum_{m=0}^{M-1}|w_m(k)|^2.\end{aligned} \tag{47}$$

Hence,

$$\left(\sigma_{\mu}^{MC}\right)^2 = \frac{N_0}{T_c}\frac{1}{SF} \times \left[\begin{aligned}&\frac{1}{SF}\sum_{k=nSF}^{(n+1)SF-1}\sum_{m=0}^{M-1}|w_m(k)|^2 + \left(\frac{U-1}{SF}\frac{E_s}{N_0}\right) \\ &\left\{\frac{1}{SF}\sum_{k=nSF}^{(n+1)SF-1}\left|\hat{H}(k)\right|^2 - \left|\frac{1}{SF}\sum_{k=nSF}^{(n+1)SF-1}\hat{H}(k)\right|^2\right\}\end{aligned}\right]. \tag{48}$$

The conditional SINR corresponding to Eq. (32) of MC-CDMA is given by

$$\gamma^{MC}\left(\frac{E_s}{N_0}, \{H_m(k)\}\right) = \frac{2\left(\frac{E_s}{N_0}\right)\left|\frac{1}{SF}\sum_{k=nSF}^{(n+1)SF-1}\hat{H}(k)\right|^2}{\left[\begin{aligned}&\frac{1}{SF}\sum_{k=nSF}^{(n+1)SF-1}\sum_{m=0}^{M-1}|w_m(k)|^2 + \left(\frac{U-1}{SF}\frac{E_s}{N_0}\right) \\ &\left\{\frac{1}{SF}\sum_{k=nSF}^{(n+1)SF-1}\left|\hat{H}(k)\right|^2 - \left|\frac{1}{SF}\sum_{k=nSF}^{(n+1)SF-1}\hat{H}(k)\right|^2\right\}\end{aligned}\right]}. \tag{49}$$

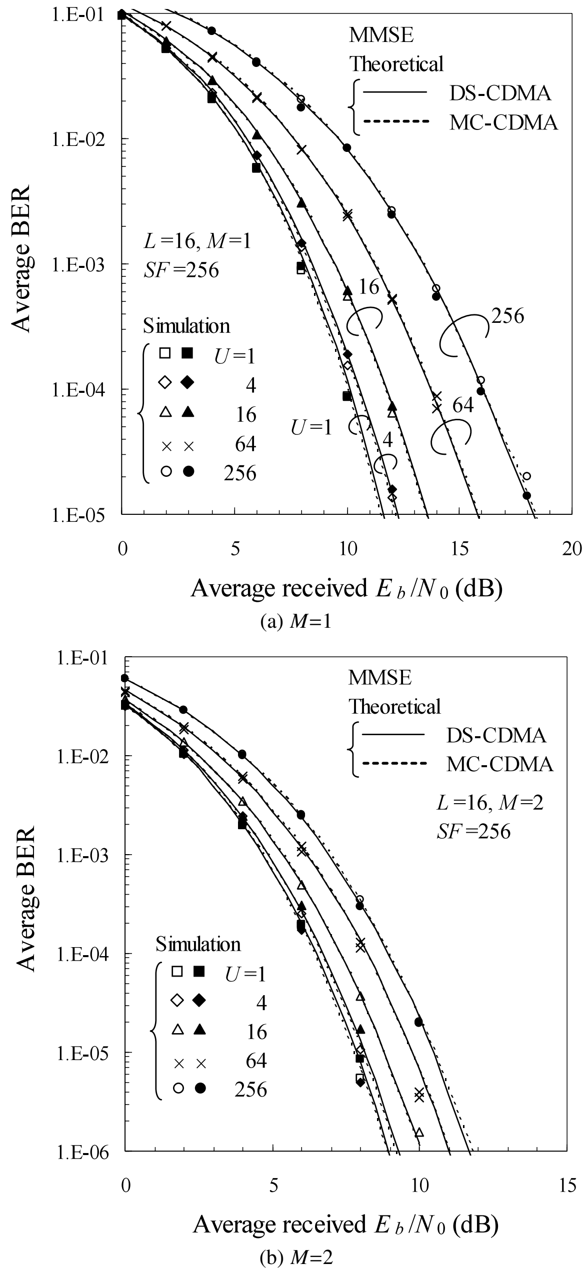

Fig. 4 Performance comparison between DS- and MC-CDMA using MMSE equalization with U as a parameter for the case of SF=256. (a) M=1 and (b) M=2.

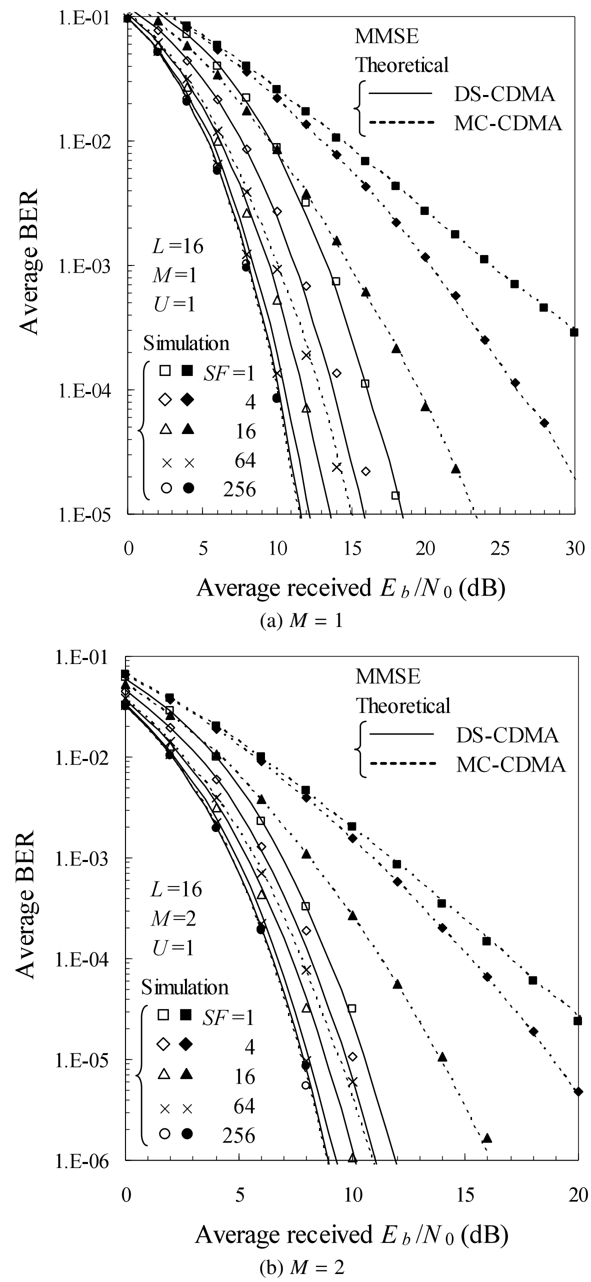

Fig. 5 Performance comparison between DS- and MC-CDMA using MMSE equalization with SF as a parameter for the case of U=1. (a) M=1 and (b) M=2.

The conditional BER is expressed as Eq. (31) and the theoretical average BER performance is numerically evaluated using Eq. (34).

When U/SF is very small, the effect of ICI (inter-code interference for MC-CDMA and inter-chip interference for DS-CDMA) is negligible and then, both MMSE and MRC equalizations provide almost the same performance. Let assume MRC equalization (i.e., $w_m(k) = H_m^*(k)$ and thus, $\hat{H}(k) = \sum_{m=0}^{M-1} |H_m(k)|^2$). When $U/SF \ll 1$, the approximate SINR with MRC equalization is given, from Eqs. (32) and (49), by

$$\gamma\left(\frac{E_s}{N_0}, \{H_m(k)\}\right) \approx \begin{cases} 2\left(\dfrac{E_s}{N_0}\right)\dfrac{1}{N_c}\displaystyle\sum_{k=0}^{N_c-1}\sum_{m=0}^{M-1}|H_m(k)|^2, \text{ for DS-CDMA} \\ 2\left(\dfrac{E_s}{N_0}\right)\dfrac{1}{SF}\displaystyle\sum_{k=nSF}^{(n+1)SF-1}\sum_{m=0}^{M-1}|H_m(k)|^2, \text{ for MC-CDMA} \end{cases}. \tag{50}$$

It can be understood from Eq. (50) that when $U/SF \ll 1$, the BER performance of DS-CDMA becomes close to its lower bound (see discussion in Sect. 4.2). When SF=N_c, the BER performances of DS- and MC-CDMA become the same (see Eqs. (32) and (49) and also see Eq. (50)). This is clearly seen in Fig. 4 which compares the average BER performances of DS- and MC-CDMA both with MMSE equalization for the case of SF=N_c=256. Again a fairly good agreement between the theoretical and the simulation results is observed.

The performance comparison between DS- and MC-CDMA for the different values of SF is shown in Fig. 5 for the case of U=1. It is seen that as SF decreases, the BER performances of both DS- and MC-CDMA degrade; however, DS-CDMA provides much better BER performance than MC-CDMA when $SF \ll N_c$ (e.g., SF=1, 4, 16). This is due to larger frequency diversity effect obtained in DS-CDMA than in MC-CDMA. In DS-CDMA, since the data symbol is always spread over all subcarriers, yielding large frequency diversity effect irrespective of SF. This results in smaller variations in γ for DS-CDMA than for MC-CDMA. This can be understood by observing Eq. (50). The reason for degrading performance with decreasing SF in DS-CDMA is due only to increasing ICI (see Eq. (29)). In MC-CDMA, as said earlier, no interference is present when U=1; however, since the data symbol is spread over smaller number (equal to SF) of subcarriers than in DS-CDMA, the frequency diversity effect is smaller and furthermore it decreases as SF reduces. However, note that performance difference diminishes as SF approaches N_c. Again observed is a good agreement between the theoretical and the simulation results.

It can also be seen from Figs. 4 and 5 that the use of antenna diversity is powerful to improve the BER performance similarly for both DS- and MC-CDMA.

As shown in Fig. 5, when $SF \ll N_c$, DS-CDMA provides much better BER performance than MC-CDMA irrespective of antenna diversity reception. However, it should be pointed out that this better BER performance of DS-CDMA is obtained at the cost of wider bandwidth than MC-CDMA; the DS-CDMA signal bandwidth is (1+α) times wider than that of MC-CDMA (although the 3 dB bandwidth is the same), where α is the roll-off factor of the square-root Nyquist chip shaping filter used at the transmitter.

5. Conclusion

In this paper, theoretical foundation was developed for joint frequency-domain equalization (FDE) and antenna diversity combining for the reception of DS-CDMA signals in a frequency-selective fading channel. Equalization weights for joint FDE and antenna diversity combining based on maximal ratio combining (MRC), zero-forcing (ZF), and minimum mean square error (MMSE) were derived. It was pointed out that FDE using MRC is equivalent to rake combining. Then, the expression for theoretical conditional bit error rate (BER) for the given set of path gains was derived by using the Gaussian approximation of inter-chip interference (ICI).

The numerical computation results on the theoretical average BER performance were presented to show that the MMSE equalization provides the best BER performance among three equalization schemes. When U=1, the BER performance is almost identical for MRC and MMSE equalizations and the E_b/N_0 degradation for achieving BER=10^{-4} from the lower bound average BER performance curve becomes as small as 0.65 dB. As U increases, the BER performance degrades since the amount of ICI increases. For large values of U, BER floors are produced in the MRC equalization due to large ICI resulting from enhanced frequency-selectivity; however, this is not produced in the MMSE and ZF equalizations. The use of antenna diversity combining was found to be powerful to improve the BER performance for all equalization schemes.

Also presented in this paper was the performance comparison between DS- and MC-CDMA. It was shown that when SF=N_c, DS-CDMA yields the same performance as MC-CDMA. When $SF \ll N_c$, DS-CDMA provides much better performance than MC-CDMA; however, performance difference diminishes as SF approaches N_c.

The theoretical results were compared with the computer simulation results. A fairly good agreement between the theoretical and the simulation results was seen.

In this paper, we considered uncoded DS- and MC-CDMA with QPSK data modulation. Channel coding can improve significantly the BER performance for both DS- and MC-CDMA. Recently, we have shown that when $U = SF = N_c$, almost identical BER performance is obtained for both coded DS- and MC-CDMA [18]. For MC-CDMA, as SF reduces, the frequency diversity effect becomes smaller, but larger frequency interleaving effect is obtained. On the other hand, for DS-CDMA, the same frequency diversity effect is obtained for all values of SF, but no frequency interleaving effect is obtained. This leads to different coding gain for DS- and MC-CDMA and the coding gain may depend on modulation level (e.g., QPSK, 16QAM and 64QAM), channel frequency-selectivity, etc. Performance analysis of coded DS- and MC-CDMA with higher level modulation is an important issue and is left as an interesting future study. Furthermore, in this paper, ideal channel estimation was assumed. The impact of the channel estimation errors on the achievable BER performances of the joint FDE and antenna diversity combining is left as another interesting study.

References

[1] F. Adachi, “Wireless past and future—Evolving mobile communications systems,” IEICE Trans. Fundamentals, vol.E84-A, no.1, pp.55–60, Jan. 2001.

[2] W.C. Jakes, Jr., ed., Microwave mobile communications, Wiley, New York, 1974.

[3] J.G. Proakis, Digital communications, 2nd ed., McGraw-Hill, 1995.

[4] F. Adachi, M. Sawahashi, and H. Suda, “Wideband DS-CDMA for next generation mobile communications systems,” IEEE Commun. Mag., vol.36, no.9, pp.56–69, Sept. 1998.

[5] S. Hara and R. Prasad, “Overview of multicarrier CDMA,” IEEE Commun. Mag., vol.35, no.12, pp.126–144, Dec. 1997.

[6] S. Hara and R. Prasad, “Design and performance of multicarrier CDMA system in frequency-selective Rayleigh fading channels,”

IEEE Trans. Veh. Technol., vol.48, no.5, pp.1584–1595, Sept. 1999.
[7] L. Hanzo, W. Webb, and T. Keller, Single- and multi-carrier quadrature amplitude modulation, John Wiley & Sons, 2000.
[8] M. Helard, R. Le Gouable, J.-F. Helard, and J.-Y. Baudais, "Multicarrier CDMA techniques for future wideband wireless networks," Ann. Telecommun., vol.56, pp.260–274, 2001.
[9] H. Atarashi, S. Abeta, and M. Sawahashi, "Variable spreading factor-orthogonal frequency and code division multiplexing (VSF-OFCDM) for broadband packet wireless access," IEICE Trans. Commun., vol.E86-B, no.1, pp.291–299, Jan. 2003.
[10] D. Falconer, S.L. Ariyavisitakul, A. Benyamin-Seeyar, and B. Eidson, "Frequency domain equalization for single-carrier broadband wireless systems," IEEE Commun. Mag., vol.40, no.4, pp.58–66, April 2002.
[11] F. Adachi, T. Sao, and T. Itagaki, "Performance of multicode DS-CDMA using frequency domain equalisation in frequency-selective fading channel," Electron. Lett., vol.39, no.2, pp.239–241, Jan. 2003.
[12] K. Takeda, T. Itagaki, and F. Adachi, "Frequency-domain equalization for antenna diversity reception of DS-CDMA signals," Proc. 8th International Conference on Cellular and Intelligent Communications (CIC), Session B3, p.383, Seoul, Korea, Oct. 2003,
[13] F. Adachi and T. Itagaki, "Frequency-domain rake combining for antenna diversity reception of DS-CDMA signals," IEICE Trans. Commun., vol.E86-B, no.9, pp.2781–2784, Sept. 2003.
[14] F. Adachi and T. Sao, "Joint antenna diversity and frequency-domain equalization for multi-rate MC-CDMA," IEICE Trans. Commun., vol.E86-B, no.11, pp.3217–3224, Nov. 2003
[15] M. Schwartz, W.R. Bennett, and S. Stein, Communication systems and techniques, McGraw-Hill, New York, 1966.
[16] T. Itagaki and F. Adachi, "Joint frequency-domain eqalization and antenna diversity combining for orthogonal multicode DS-CDMA signal transmissions in a frequency-selective fading channel," Proc. 6th International Symposium on Wireless Personal Multimedia Communications (WPMC), vol.1, pp.285–289, Yokosuka, Japan, Oct. 2003.
[17] A. Chouly, A. Brajal, and S. Jourdan, "Orthgonal multicarrier techniques applied to direct sequence spread spectrum CDMA system," Proc. IEEE Globecom'93, pp.1723–1728, Nov. 1993.
[18] D. Garg and F. Adachi, "Performance comparison of turbo coded MC-CDMA and DS-CDMA with higher level modulation," Proc. IEICE Gen. Conf. 2004, SB-9-2, March 2004.

Appendix: Derivation of σ^2_{ICI} and σ^2_{noise} for DS-CDMA

Since $E[c(t)c^*(\tau)] = \delta(t-\tau)$, we have

$$\sigma^2_{ICI} = \frac{1}{SF^2N_c^2}\frac{E_c}{T_c}\sum_{t=nSF}^{(n+1)SF-1}\sum_{k=0}^{N_c-1}\sum_{k'=0}^{N_c-1}\hat{H}(k)\hat{H}^*(k') \times\left[\sum_{\substack{\tau=0\\ \neq t}}^{N_c-1}\sum_{\substack{\tau'=0\\ \neq t}}^{N_c-1}E[s(\tau)s^*(\tau')]\exp\left(j2\pi k\frac{t-\tau}{N_c}-j2\pi k'\frac{t-\tau'}{N_c}\right)\right]. \tag{A· 1}$$

The DS-CDMA signal using the scramble sequence together with orthogonal spreading sequences is white-noise like and hence, $E[s(\tau)s^*(\tau')] = U\delta(\tau-\tau')$. Therefore, Eq. (A· 1) becomes

$$\begin{aligned}\sigma^2_{ICI} &= \frac{U}{SF^2N_c^2}\frac{E_c}{T_c}\sum_{t=nSF}^{(n+1)SF-1}\sum_{k=0}^{N_c-1}\sum_{k'=0}^{N_c-1}\hat{H}(k)\hat{H}^*(k') \\ &\quad\times\left[\sum_{\substack{\tau=0\\ \neq t}}^{N_c-1}\exp\left(j2\pi(k-k')\frac{t-\tau}{N_c}\right)\right] \\ &= \frac{U}{SF^2N_c^2}\frac{E_c}{T_c}\sum_{t=nSF}^{(n+1)SF-1}\sum_{k=0}^{N_c-1}\sum_{k'=0}^{N_c-1}\hat{H}(k)\hat{H}^*(k') \\ &\quad\times\left[\sum_{\tau=0}^{N_c-1}\exp\left(j2\pi(k-k')\frac{t-\tau}{N_c}\right)-1\right].\end{aligned} \tag{A· 2}$$

Since

$$\sum_{\tau=0}^{N_c-1}\exp\left(j2\pi(k-k')\frac{t-\tau}{N_c}\right) = N_c\delta(k-k'), \tag{A· 3}$$

we obtain

$$\begin{aligned}&\sigma^2_{ICI} \\ &\quad= \frac{U}{SF}\frac{E_c}{T_c}\frac{1}{N_c^2}\sum_{k=0}^{N_c-1}\sum_{k'=0}^{N_c-1}\hat{H}(k)\hat{H}^*(k')\left[N_c\delta(k-k')-1\right] \\ &\quad= \frac{U}{SF}\frac{E_c}{T_c}\left[\frac{1}{N_c}\sum_{k=0}^{N_c-1}\left|\hat{H}(k)\right|^2-\left|\frac{1}{N_c}\sum_{k=0}^{N_c-1}\hat{H}(k)\right|^2\right].\end{aligned} \tag{A· 4}$$

Next, we obtain σ^2_{noise}. Since $E[c(t)c*(\tau)] = \delta(t-\tau)$, we have

$$\begin{aligned}\sigma^2_{noise} &= \frac{1}{SF^2N_c^2}\sum_{t=nSF}^{(n+1)SF-1}\times\sum_{k=0}^{N_c-1}\sum_{k'=0}^{N_c-1}E[\hat{\Pi}(k)\hat{\Pi}^*(k')] \\ &\qquad\exp\left(j2\pi(k-k')\frac{t}{N_c}\right).\end{aligned} \tag{A· 5}$$

Since $\{\Pi_m(k);\ m = 0 \sim M-1 \text{ and } k = 0 \sim N_c-1\}$ are zero-mean and i.i.d. complex-valued Gaussian variables having a variance of $2(N_0/T_c)N_c$, $\{\hat{\Pi}(k);\ k = 0 \sim N_c-1\}$ become also zero-mean and i.i.d. complex-valued Gaussian variables and thus, we have

$$\sigma^2_{noise} = \frac{1}{SF}\frac{N_0}{T_c}\left(\frac{1}{N_c}\sum_{k=0}^{N_c-1}\sum_{m=0}^{M-1}|w_m(k)|^2\right). \tag{A· 6}$$

Fumiyuki Adachi received his B.S. and Dr.Eng. degrees in electrical engineering from Tohoku University, Sendai, Japan, in 1973 and 1984, respectively. In April 1973, he joined the Electrical Communications Laboratories of Nippon Telegraph & Telephone Corporation (now NTT) and conducted various types of research related to digital cellular mobile communications. From July 1992 to December 1999, he was with NTT Mobile Communications Network, Inc. (now NTT DoCoMo, Inc.), where he led a research group on wideband/broadband CDMA wireless access for IMT-2000 and beyond. Since January 2000, he has been with Tohoku University, Sendai, Japan, where he is a Professor of Electrical and Communication Engineering at Graduate School of Engineering. His research interests are in CDMA and TDMA wireless access techniques, CDMA spreading code design, Rake receiver, transmit/receive antenna diversity, adaptive antenna array, bandwidth-efficient digital modulation, and channel coding, with particular application to broadband wireless communications systems. From October 1984 to September 1985, he was a United Kingdom SERC Visiting Research Fellow in the Department of Electrical Engineering and Electronics at Liverpool University. From April 1997 to March 2000, he was a visiting Professor at Nara Institute of Science and Technology, Japan. He was a recipient of IEICE Achievement Award 2002 and was a co-recipient of the IEICE Transactions best paper of the year award 1996 and again 1998. He is an IEEE Fellow and was a co-recipient of the IEEE Vehicular Technology Transactions best paper of the year award 1980 and again 1990 and also a recipient of Avant Garde award 2000.

Kazuaki Takeda received his B.E. degree in communications engineering from Tohoku University, Sendai, Japan, in 2003. Currently he is a graduate student at the Department of Electrical and Communications Engineering, Graduate School of Engineering, Tohoku University. His research interests include frequency-domain equalization for direct sequence CDMA and transmit/receive diversity techniques.